F., and Chambon, P. (1970), *Biochem. Biophys. Res. Commun. 38*, 165.
Kuntzel, H., and Schafer, K. P. (1971), *Nature (London), New Biol. 231*, 265.
Low, B. W. (1952), *J. Amer. Chem. Soc. 74*, 4830.
Lowry, O. H., Rosebrough, N. J., Farr, A. L., and Randall, R. J. (1951), *J. Biol. Chem. 193*, 256.
Luck, D. J. K., and Reich, E. (1964), *Proc. Nat. Acad. Sci. U. S. 52*, 931.
Mukerjee, H., and Goldfeder, A. (1972), *Fed. Proc., Fed. Amer. Soc. Exp. Biol. 31* (2), 310.
Neubert, D., and Helge, H. (1965), *Biochem. Biophys. Res. Commun. 18*, 600.
Novello, F., and Stirpe, F. (1970), *FEBS (Fed. Eur. Biochem. Soc.) Lett. 8*, 57.
O'Brien, T. W., and Kalf, G. F. (1967), *J. Biol. Chem. 242*, 2172.
Reid, B. D., and Parsons, P. (1971), *Proc. Nat. Acad. Sci. U. S. 68*, 2830.
Roeder, R. G., and Rutter, W. J. (1969), *Nature (London) 224*, 234.
Roodyn, D. B., and Wilkie, D. (1968), The Biogenesis of Mitochondria, London, Methuen and Co. Ltd.
Saccone, C., and Gadaleta, M. N. (1970), Abstracts of the 8th International Congress of Biochemistry, Geneva, Switzerland, No. 185.
Samejima, T., Kamata, M., and Shibata, K. (1962), *J. Biochem. (Tokyo) 51*, 181.
Shmerling, Zh. G. (1969), *Biochem. Biophys. Res. Commun. 37*, 965.
Slater, E. C., Tager, J. S., Papa, S., and Quagliarello, E. (1968), *Biochem. Aspects Biogenesis Mitochondria, Proc. Round Table Discuss.*, 380.
Suyama, Y., and Eyer, J. (1968), *J. Biol. Chem. 243*, 320.
Tsai, M., Michaelis, G., and Criddle, R. S. (1971), *Proc. Nat. Acad. Sci. U. S. 68*, 473.
Umezawa, H., Mizuno, S., Yamazaki, U., and Nitta, K. (1968), *J. Antibiot., Ser. B 21*, 234.
Weber, K., and Osborn, M. (1969), *J. Biol. Chem. 244*, 4406.
Wehrli, W., Knusel, F., and Staehelin, M. (1968a), *Biochem. Biophys. Res. Commun. 32*, 284.
Wehrli, W., Nuesch, J., Knusel, F., and Staehelin, M. (1968b), *Biochim. Biophys. Acta 157*, 215.
Wintersberger, E. (1964), *Hoppe-Seyler's Z. Physiol. Chem. 336*, 285.
Wintersberger, E., and Wintersberger, U. (1970), *FEBS (Fed. Eur. Biochem. Soc.) Lett. 6*, 58.
Wu, G., and Dawid, I. B. (1972), *Biochemistry 11*, 3589.

Conformation of Nicotinamide Adenine Dinucleotide Bound to Cytoplasmic Malate Dehydrogenase†

Lawrence E. Webb, Edward J. Hill,‡ and Leonard J. Banaszak*,§

ABSTRACT: The structure of NAD^+ bound to each subunit of cytoplasmic malate dehydrogenase has been determined from an electron density map at 2.5-Å resolution. The structures of the bound coenzyme molecules are closely related by the two-fold rotational symmetry of the dimeric enzyme with the binding sites at the closest point about 20 Å apart. The NAD^+ molecule is in an open conformation with the bases unstacked. The torsion angles are in general agreement with those found in 5′-nucleotides and polynucleotides, with the exception of differences in ribose ring and phosphate orientation, which presumably accommodate binding to the protein. An isolated electron density peak, ascribed to a sulfate ion, is located close to the nicotinamide ring in a position which could be the substrate location during catalysis. The coenzyme structure and binding are very similar to those found crystallographically in lactate dehydrogenase, but some differences are observed. One segment of protein chain, which forms a loop near the coenzyme, is shifted relative to the coenzyme in one of the malate dehydrogenase subunits. This shift differs from the folding down of the same segment observed in the abortive ternary complex of lactate dehydrogenase.

Nicotinamide adenine dinucleotide, NAD^+, along with its 2′-phosphoric acid derivative, $NADP^+$, are coenzymes in a very large number of enzymatic oxidations and reductions. A simple example of this form of metabolic reaction is the oxidation of hydroxy acids

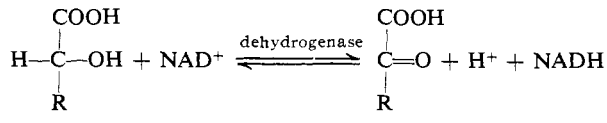

For the enzyme, malate dehydrogenase, R is $\cdot CH_2COOH$, and for lactate dehydrogenase, R is $\cdot CH_3$. In the direction of oxidation, two hydrogen atoms are removed from the carboxylic acid. One hydrogen atom plus one electron are transferred to the 4 position of the nicotinamide ring and one proton is found in the solvent.[1] Figure 1 shows the covalent struc-

† From the Department of Biological Chemistry, Washington University School of Medicine, St. Louis, Missouri 63110. *Received June 18, 1973.* This work was supported by grants from the National Science Foundation (GB-27437X), National Institutes of Health (GM-13925), and the Life Insurance Medical Research Fund (G-70-26).

‡ Postdoctoral fellow of the National Institutes of Health (1-F02-GM 49896-01). Present address: Department of Physiology, Vanderbilt University Medical School, Nashville, Tenn.

§ Research Career Development awardee of the National Institutes of Health (GM-14357).

[1] For a discussion of the chemistry of NAD^+ as related to dehydrogenases, see Bruice and Benkovic (1966).

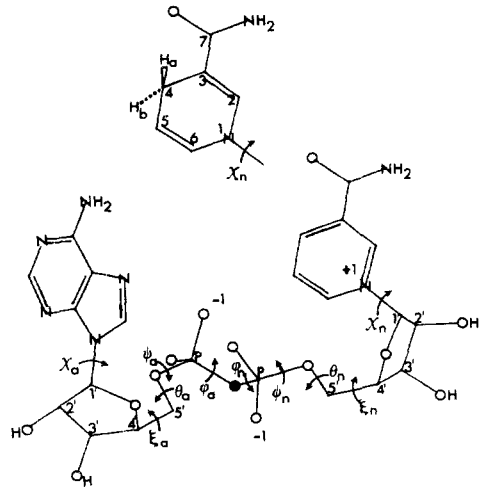

FIGURE 1: Covalent structure of nicotinamide adenine dinucleotide showing torsion angles as defined by Arnott and Hukins (1969). The atom referred to as the bridge oxygen atom is shown as a black circle. All models and electron density contours included in figures in this paper are reproduced directly from a molecular modeling system cathode ray tube display (Hill *et al.*, 1972).

ture of NAD^+, the pyridine ring in the reduced form, and the nomenclature which will be used in the subsequent discussion.

The hydrogen (or hydride ion) may be transferred to C-4 of the nicotinamide ring in two sterically distinguishable positions, either to the position labeled H_A or H_B. This gives rise to two classes of dehydrogenases, type A and type B. Cytoplasmic malate dehydrogenase from pig heart (Davies *et al.*, 1972) and muscle lactate dehydrogenase (Levy and Vennesland, 1957) are type A dehydrogenases. The two different sides of the nicotinamide ring are shown in the reduced nicotinamide ring in Figure 1.

Detailed structural information on the conformation of both cytoplasmic malate dehydrogenase from pig heart (Hill *et al.*, 1972) and dogfish muscle lactate dehydrogenase (Adams *et al.*, 1970a; Rossman *et al.*, 1971) has been obtained by X-ray analysis. Since all dehydrogenases involve at least two substrates, NAD^+, and in the case of malate dehydrogenase, the dicarboxylic acid, multiple binding steps must occur in the catalytic reaction. The general terminology which has evolved describes the apoenzyme with bound NAD^+ as a binary complex, or the enzyme with bound NAD^+ and the other substrate or substrate analog as a ternary complex. The native crystals of malate dehydrogenase contain bound NAD^+ and therefore represent some form of a binary complex (Glatthaar *et al.*, 1972). Dogfish lactate dehydrogenase in the principle crystalline form is the apoenzyme (Adams *et al.*, 1970a).

Since this report describes preliminary information on the location of the NAD^+ binding site in malate dehydrogenase and the conformation of this bound NAD^+, Figure 1 also illustrates the conformational degrees of freedom of the dinucleotide. To make possible easy comparison with the lactate dehydrogenase results, the torsion angles which define these degrees of freedom are labeled according to the system of Arnott and Hukins (1969), with positive rotations always in a clockwise direction looking down the indicated bond. Not shown in Figure 1 is the puckering of the ribose ring. It will be assumed that in the NAD^+, ribose puckering is either C-2′- or C-3′-endo (Arnott and Hukins, 1969). This simply means that the C-2′ or C-3′ atom deviates most from the least-squares plane of the ribose ring and the deviation is in the direction of the C-5′ atom (Sundaralingam, 1973).

Since the nature of any charged group on NAD^+ would probably affect binding to malate dehydrogenase, such groups are also shown in Figure 1. Note that the positive charge on the nicotinamide ring does not involve an ionizable group in the normal pH ranges and that it is absent in the reduced form, NADH. The pK of the adenine amino group is about 4 so that it is probably neutral at pH 5.0 where the malate dehydrogenase structure has been studied. The two ionizable OH groups attached to the two phosphorus atoms in the diester linkage have low pK values (<2) and are both likely to have negative charges at the pH used in this study.

The asymmetric unit of malate dehydrogenase crystals contains the dimeric molecule with the two subunits arranged so that they are related by an approximate twofold rotation axis (Hill *et al.*, 1972), which we shall call the molecular dyad. Although the polypeptide conformation is known from the studies at 3.0-Å resolution, detailed information on the amino acid sequence is not yet available. Atomic coordinates up to and including the β carbons have been determined for only one subunit. It must therefore be emphasized that subtle conformational differences may exist between the two subunits. The possibility of these differences was first suggested by studies at 5.0-Å resolution. For example, when the native crystals were soaked in high concentrations of NAD^+ and then studied by difference Fourier methods, additional electron density was found. However, these changes were associated with only one subunit, which we shall call subunit 2 (Tsernoglou *et al.*, 1971). This low resolution study pointed to the region of the malate dehydrogenase molecule which should contain one of the NAD^+ binding sites. The position of the other, in subunit 1, was inferred from the molecular symmetry (Hill *et al.*, 1972). In the map of the native protein at 2.5-Å resolution, it became clear that electron density belonging to NAD^+ was present in both subunits. The additional electron density which was observed by difference Fourier methods at low resolution, and recently in a 2.5-Å resolution difference map, probably results from the fact that the occupancy at this one site, in subunit 2, is increased by soaks in very high concentrations of NAD^+. These interpretations of the location of the NAD^+ binding site are in good agreement with the binding site described for dogfish lactate dehydrogenase (Adams *et al.*, 1970a,b).

Experimental Methods

X-Ray diffraction data were extended from 3.0- to 2.5-Å resolution, employing the heavy atom derivatives and anomalous scattering measurements described previously (Hill *et al.*, 1972). The crystals were again prepared with a tenfold molar excess of NAD^+.

The 2.5-Å electron density map was computed from a total of 74,497 independent reflections. The unit cell grid intervals for each section of the map were 128 along a and 64 along b. The 64 sections were spaced at intervals of 0.92 Å along c and were contoured for model building of the complete polypeptide backbone in an optical comparator using a half-silvered mirror (Richards, 1968). The highest integrated electron densities were found in two continuous envelopes of density, one in each subunit, which could not be attributed to any part of the peptide backbone or its side chains. These envelopes were assigned to the bound dinucleotide, and sections containing them, together with neighboring electron density, were selected for coenzyme model building in a smaller comparator.

For each subunit, coordinates for many different conformations of the coenzyme were measured in the optical compara-

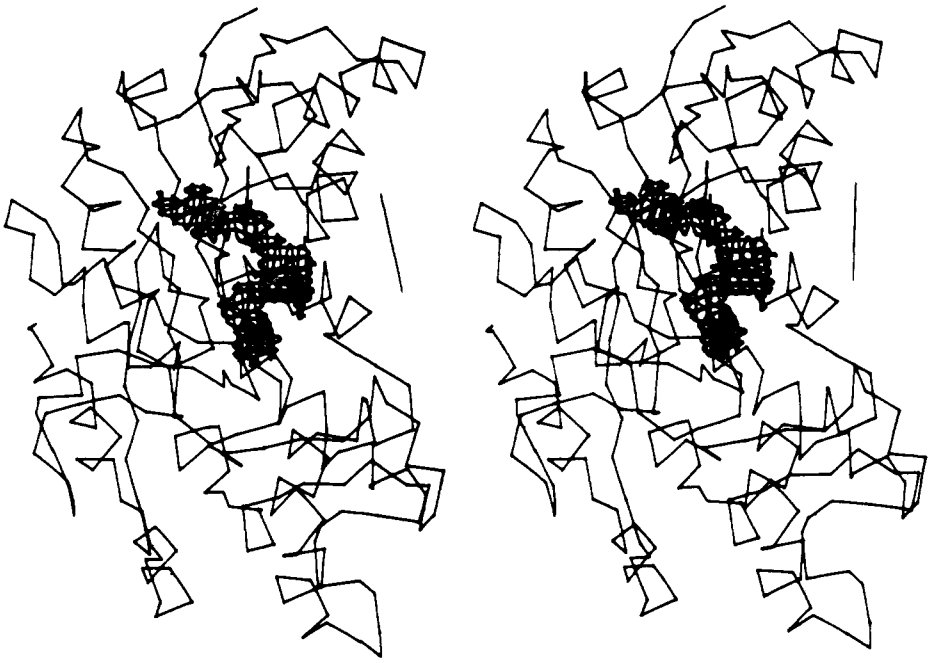

FIGURE 2: Stereoview of an α-carbon model of malate dehydrogenase subunit 1 and the portion of the 2.5-Å electron density map of this subunit which contains the bound dinucleotide. A single arbitrary contour level is plotted on orthogonal sections.

tor and entered into the molecular modeling system (Hill *et al.*, 1972). This was done by building dinucleotide conformations which still fitted the electron density but had variations in the torsional angles. This computer interactive display system permitted each model to be examined in stereo superimposed on a selected volume of electron density contours. Three-dimensional perception was enhanced by the simultaneous display of two orthogonal sets of contours which could be rotated together with the model.

The measured model was not altered but was used as a guide to be followed closely while fitting the density with another displayed NAD^+ model which incorporated standard bond lengths and bond angles. This standard model was constructed initially in an arbitrary conformation with the molecular modeling system. The final models were obtained by varying the previously described torsion angles, and rigid body rotations and translations. These parameters were altered one at a time while watching the display of the model in the electron density.

The molecular dimensions of the standard model were taken from the fundamental nucleotide units (C-3′-endo and C-2′-endo) derived from X-ray crystal-structure determinations of nucleosides, nucleotides, and dinucleoside monophosphates (Sundaralingam, 1973). It is worth noting that the angle at the phosphorus atom involving the ester oxygens was decreased from the tetrahedral value to 101°, in accordance with values obtained from triphosphates, phosphodiesters, and the only crystal structure of an organic pyrophosphate thus far reported (Pletcher and Sax, 1966; Sundaralingam, 1969). The derivation of the detailed conformation of the bound dinucleotide is described below.

Results and Discussion

The location of the coenzyme electron density in subunit 1 relative to an α-carbon model of malate dehydrogenase is shown in Figure 2. The adenine end of the dinucleotide fits tightly into a crevice near the surface, and the nicotinamide end extends deep into a cavity in the interior of the enzyme. The NAD^+ site in the other subunit is related by the molecular dyad and is separated from the site shown in Figure 2 by about 20–25 Å.

Derivation of NAD^+ Conformation. Several prominent features of the electron density map served as starting points in deriving the conformation of the dinucleotide in each subunit. The two phosphorus atoms were kept as close as possible to two peaks in the central region of the coenzyme densities. These electron density maxima were among the highest in the entire map. One of the nicotinamide phosphate oxygens in subunit 1 was clearly delineated in the map, although the other phosphorus oxygens were poorly resolved. Further guidance was provided by protuberances of electron density which were assumed to be ribose oxygens hydrogen bonded to the protein. Examination of the density contours at suitable orientations in the molecular modeling system display clearly delineated the location and orientation of the planar adenine rings.

An attempt was made to build all models with torsion angles which were as close as possible to "expected" values, without sacrificing the fit to the electron density. The expected values were based on surveys of known crystal structures (Arnott and Hukins, 1969; Sundaralingam, 1969, 1973). In the final model, deviations from these values were not allowed if van der Waals distances were violated. Many earlier models followed the main features of the electron density but had some sterically unreasonable torsion angles.

When the full range of allowed pyrophosphate conformations was taken into account, it became possible to build a model with a better fit to the electron density with torsion angles much closer to those previously observed in other dinucleotides. Within the restrictions imposed by the previously observed staggering of the phosphate oxygens when viewed down the P–P axis (Sundaralingam, 1969), a large number of pyrophosphate conformations differing in the orientation of the bridge oxygen atom are possible. Some of these conformations are depicted in Figure 3. It became clear that the con-

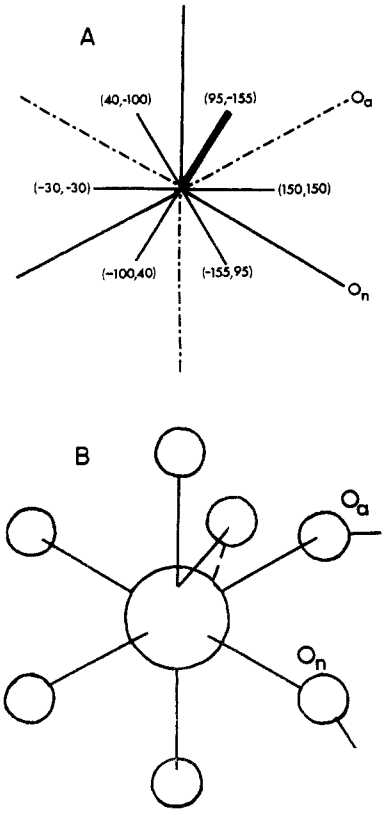

FIGURE 3: (A) Schematic diagram of possible staggered pyrophosphate conformations viewed down the P–P axis. (B) Conformation selected for NAD^+ bound to malate dehydrogenase. In this view, the position of the pyrophosphate bridge oxygen is usually found to project midway between two of the hexagonally distributed oxygens (Sundaralingam, 1969; Pletcher and Sax, 1966). The ester oxygens bonded to the nicotinamide and adenine ribose rings are labeled O_n and O_a, respectively. The six projected bridge oxygen positions which fulfill the staggering conditions for the selected positions of O_n and O_a are shown in A with the dihedral angles ϕ_n and ϕ_a given in parentheses. These angles are defined in Figure 1. Their suggested values are not exact but suggest angular ranges of 20–30° which give the staggering shown with the assumed NAD^+ pyrophosphate structure discussed in the text. The considerable distortion from tetrahedral geometry at each phosphorus atom precludes a more precise definition of each staggered position. The position tentatively chosen for the NAD^+ bridge oxygen in both malate dehydrogenase subunits is indicated by the heavy line.

formation shown in Figure 3 with the ester oxygens gauche rather than trans about the P–P axis fit the NAD^+ density best, but the location of the remaining phosphorus oxygens was not well defined in the electron density. With the adenine ring, the nicotinamide ring, and the two ribose rings fixed in relatively well-defined density at both ends of the dinucleotide, the pyrophosphate conformation was varied by changing the position of the bridge oxygen relative to the ester oxygens as depicted in Figure 3. In each subunit, the conformation which appeared to best connect the two ribose rings was selected.

Overall Structural Features. The final models for the dinucleotide bound to each subunit are shown in Figure 4 superimposed on their electron density contours. Torsion angles for these models are listed in Table I. The NAD^+ in subunit 1 (NAD1) rotated 180° about the molecular dyad and superimposed on the NAD^+ in subunit 2 (NAD2) is shown in Figure 5. The NAD1 and NAD2 structures, although derived independently, are nearly identical, and it is likely that apparent differences are not significant.

TABLE I: Torsion Angles (Degrees) for NAD^+ in Malate Dehydrogenase Binary Complex and Lactate Dehydrogenase Ternary Complex.[a]

Torsion Angle	Malate		Lactate Ternary[b]
	Subunit 1	Subunit 2	
χ_a	110	115	89
ξ_a (ψ)	−78	−74	−78
θ_a (ϕ)	−167	−150	−159
ψ_a (ω)	58	67	109
ϕ_a (ω')	−166	−156	156
ϕ_n	88	84	49
ψ_n	147	160	87
θ_n	160	150	−171
ξ_n	−40	−61	−53
χ_n	132	133	106
$Ribose_a$	C-3′-endo	C-3′-endo	C-3′-endo
$Ribose_n$	C-2′-endo	C-2′-endo	C-3′-endo

[a] The torsion angles are defined according to the conventions of Arnott and Hukins (1969) and are shown in Figure 1. To facilitate comparisons, the notation of Sundaralingam (1969) is given in parentheses where the definition of the angle is the same as that of Arnott and Hukins. [b] Abortive ternary complex (Chandrasekhar *et al.*, 1973).

Despite incomplete resolution of some of the oxygen atoms, the main features of the structure are clearly delineated in the electron density contours (Figure 4). Although the two sets of torsion angle values listed in Table I are calculated from models which fit these density contours adequately at 2.5-Å resolution, these values are not necessarily a unique solution to the density fitting problem. The NAD^+ conformation will therefore be discussed first in terms of some characteristic structural parameters shown in Figure 6 and listed in Table II.

The coenzyme is basically in an open conformation when bound to malate dehydrogenase, in contrast to the folded form which it can assume in aqueous solution (McDonald *et al.*, 1972). The adenine and nicotinamide rings are not stacked over each other but are about 15 Å apart, as shown in Figure 6. Furthermore, the angle between the adenine and nicotinamide ring planes is about 110° in NAD1 and 80° in NAD2. Although the latter two values probably have un-

TABLE II: Comparison of Intramolecular Structure Parameters for Bound NAD^+.

Distances (Å)	Malate		Lactate Ternary[a]
	Subunit 1	Subunit 2	
P_a–N-9	6.9	6.9	6.9
P_a–C-4′$_a$	4.0	3.9	3.9
P_n–N-1	6.4	6.5	6.6
P_n–C-4′$_n$	4.0	3.9	3.9
C-6$_a$–C-2$_n$	14.3	14.2	14.1
Angle (deg)			
α[b]	−80	−77	−41

[a] Coordinates taken from Chandrasekhar *et al.* (1973). [b] Dihedral angle about the P–P axis; defined in Figure 6.

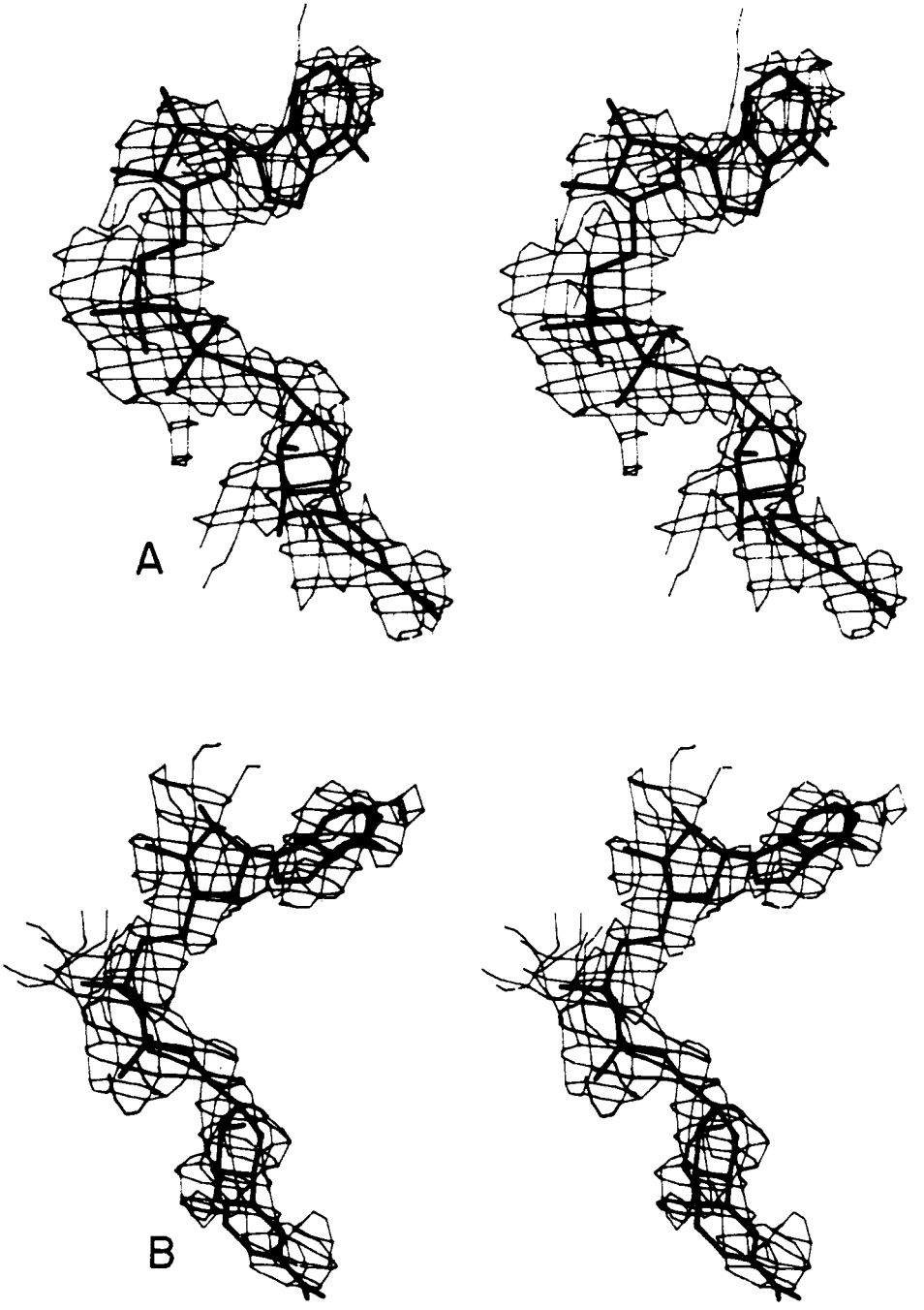

FIGURE 4: Models of NAD^+ bound to malate dehydrogenase subunit 1 (A) and to malate dehydrogenase subunit 2 (B) as fitted to the 2.5-Å resolution electron density map. Contours were generated as in Figure 2 and those belonging to neighboring protein were suppressed for clarity. The NAD^+ of subunit 1 has been rotated about the malate dehydrogenase molecular dyad for easy comparison with subunit 2.

certainties of 10–20°, they show clearly that the bases are not parallel but are nearly perpendicular. The interatomic distances given in Figure 6 show that both 5′-nucleotides in the dinucleotide have similar dimensions characteristic of an extended conformation.

It should be emphasized, however, that the coenzyme is not in a completely extended form, since there is a turn or fold at the pyrophosphate group as shown in Figure 3. The overall shape of the coenzyme can be further characterized by the dihedral angle α, defined in Figure 6. This parameter indicates that the adenine ring is rotated counterclockwise about the P–P axis about 80° with respect to the nicotinamide ring.

Conformational Analysis. The suggested values of torsion angles in Table I have the same pattern for the two nucleotides making up the dinucleotide. Differences in the torsion angles are small and may not be significant, with the exception of the ϕ and ψ angles. There are some deviations from the expected values mentioned above (Arnott and Hukins, 1969; Sundaralingam, 1969, 1973), which were derived from structures of polynucleotides and nucleotides not bound to a protein. These deviations are no larger than about 20–30°. A determination of whether or not they are significant must await a least-squares refinement of the torsion angle variables with respect to the electron density after all protein side chain density has been interpreted.

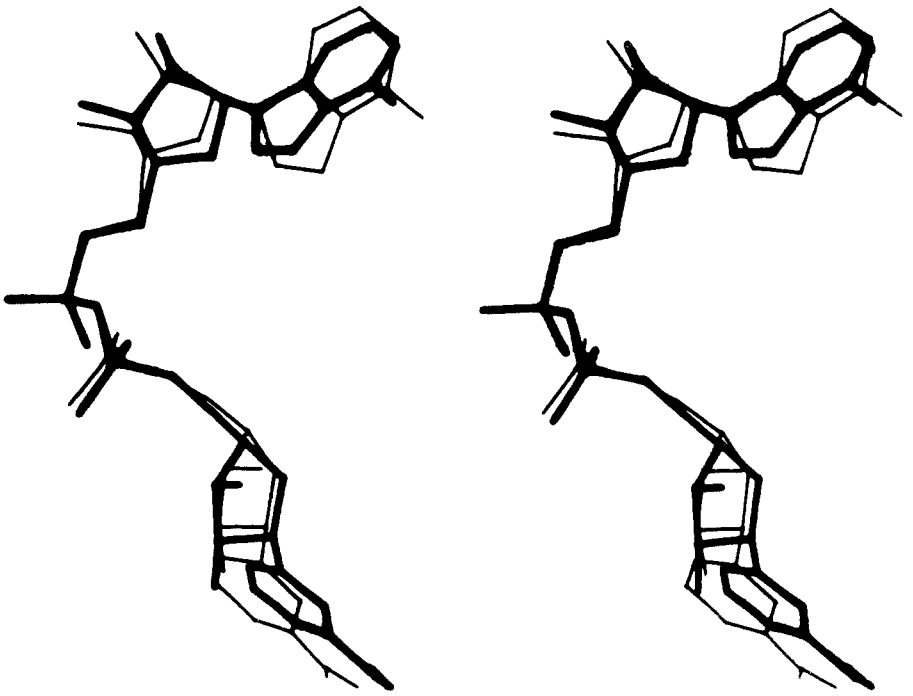

FIGURE 5: Comparison of the structures derived for NAD^- bound to subunit 1 (NAD1) and subunit 2 (NAD2) in malate dehydrogenase The heavy lines represent NAD2. NAD1 was rotated 180° about the molecular dyad (Hill *et al.*, 1972) and then translated 2.03 Å along a line between the two adenine phosphorus atoms to make these two atoms superimpose. Data are not yet available to determine if this translation reflects a significant deviation of the twofold axis relating NAD1 and NAD2 from an accurate twofold axis relating the two protein subunits.

In addition to the torsion angles listed in Table I, the angles given by Arnott and Hukins (1969) were used to build the C-3′-endo and C-2′-endo puckered ribose rings. The C-4′–C-5′ and N–C-1′ bonds for these two ribose conformations can be made to superimpose by appropriate alterations in the χ and ξ angles. Therefore, these bonds and the ribose oxygens must both be well defined for one to decide which puckering best fits the electron density. The adenine ribose rings fit the density almost equally well with either puckering. The C-3′-endo conformation was chosen because the χ angle could then be made closer to the normal range of values. The C-2′-endo conformation of the nicotinamide ribose rings was easier to build into the electron density than the C-3′-endo alternative found in NAD^+ bound to lactate dehydrogenase (Chandrasekhar *et al.*, 1973).

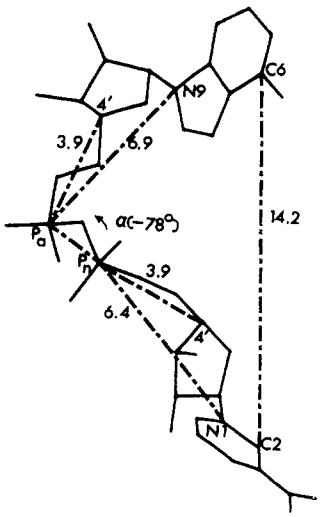

FIGURE 6: Structural parameters of NAD^+ bound to malate dehydrogenase. The figure was produced from a computer display of the structure derived for the dinucleotide bound to subunit 1. Interatomic distances shown by the dashed lines are given in Ångströms. The angle α indicated by the arrow is the dihedral angle about the P–P axis defined for the vectors N-9–P_a, P_n–P_a, and P_n–N-1 with the same conventions as for the backbone torsion angles. This angle and the distances shown are averages of the values listed in Table II for NAD^+ bound to the two malate dehydrogenase subunits.

Both bases are clearly in the anti position. The χ_a and χ_n values quoted here, although somewhat larger than the averages of χ values found in structures with purine and pyrimidine bases, are consistent with a stable conformation determined from space filling models.

A striking feature of the NAD^+ conformation when bound to malate dehydrogenase is that the staggered conformation about the C-4′–C-5′ bond is trans–gauche (ξ near $-60°$) rather than the gauche–gauche ($\xi = 60°$) conformation found in all crystal structure determinations of 5′-nucleotides and polynucleotides (Sundaralingam, 1973). The same trans–gauche conformation is found also in the lactate dehydrogenase ternary complex and may allow more hydrogen bonds to the protein than the gauche–gauche conformation. The other staggered conformation (ξ near 180°) has been found in adenosine, AMP, and ADP bound to lactate dehdyrogenase (Chandrasekhar *et al.*, 1973) and in AMP in solution (Barry *et al.*, 1971).

The pyrophosphate conformation found for both subunits is shown in Figure 3. Although the gauche arrangement of the ester oxygens is reasonably certain in both subunits, the relative position of the pyrophosphate bridge may not be the same. Higher resolution data may reveal differences which would change the ϕ and possibly the ψ values greatly. It is interesting to note that the conformation in the present

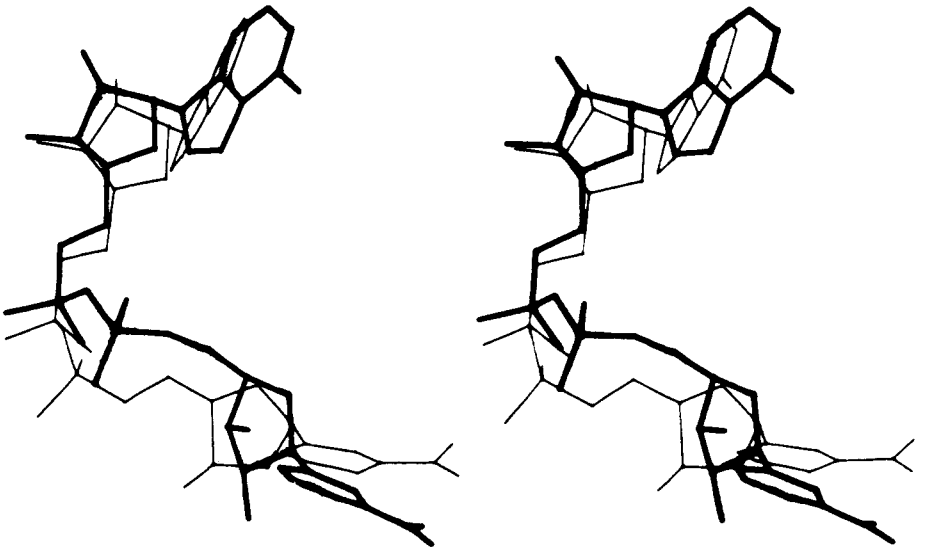

FIGURE 7: Model for NAD^+ in the abortive ternary complex lactate dehydrogenase–NAD^+–pyruvate superimposed on the model for NAD^+ bound to malate dehydrogenase subunit 2 (heavy lines). Coordinates for the ternary complex were taken from Chandrasekhar *et al.* (1973). The superposition is not a least-squares fit but was done by visual inspection of a cathode ray tube display.

interpretation of the electron density is consistent with the observations of Sundaralingam (1969) concerning phosphodiesters and the amidotriphosphate ion. He noted that in phosphodiesters an anti–gauche (tg) conformation is preferred over an anit–anti (tt) conformation, which has interference between the lone-pair orbitals on the two ester oxygens. Taking the torsional angles in Table I in the order ψ_n, ϕ_n, ϕ_a, ψ_a, one sees that the conformation about each NAD^+ phosphorus atom can be characterized as tg^+ in Sundaralingam's notation. The conformation about the pyrophosphate bridge atom, given by the angles ϕ_n and ϕ_a, can also be characterized as gauche–anti. Thus, the lone-pair orbitals on the bridge oxygen as well as those on the two ester oxygens may have a significant influence on the conformation of the dinucleotide.

Comparison with NAD^+ in Lactate Dehydrogenase. The structure of NAD^+ when bound to lactate dehydrogenase in a binary complex (Adams *et al.*, 1970b) has recently been compared to the structure of bound NAD^+ in the ternary complex lactate dehydrogenase–NAD^+–pyruvate (Chandrasekhar *et al.*, 1973). There are significant differences between coenzyme binding in these complexes, but the NAD^+ conformations are nearly the same. The structure in the ternary complex, determined from higher resolution data (Rossman *et al.*, 1971), is selected for comparison here.

Table I shows that the torsion angles for NAD^+ in the lactate dehydrogenase ternary complex and in both malate dehydrogenase subunits are very similar with the exception of the nicotinamide ribose puckerings discussed above and the pyrophosphate conformations described by the ϕ and ψ angles. These differences may not be significant, as the structures found for NAD^+ bound to malate and lactate dehydrogenase superimpose quite closely as shown by Figure 7 and the structural parameters given in Table II. Note in Figure 7 that the orientation of the phosphorus oxygen atoms is nearly the same although the ϕ and ψ angles are very different. There are obvious differences between the two NAD^+ models, however, and one way of characterizing them is the dihedral angle, α, involving rotations of the P_a–N-9 and P_n–N-1 vectors about the P–P axis. This angle is much smaller in the lactate dehydrogenase ternary complex. It is possible that this difference is only a reflection of the way the electron densities were interpreted. The close resemblance of the NAD^+ structures when bound to the two dehydrogenases is not surprising in view of the nearly homologous structures of malate dehydrogenase and dogfish lactate dehydrogenase (Hill *et al.*, 1972). Furthermore, the observed NAD^+ conformations must be closely correlated with interactions between the dinucleotide and protein, which have striking similarities in lactate and malate dehydrogenase.

These interactions in malate dehydrogenase are illustrated by the schematic diagram in Figure 8. The nomenclature for

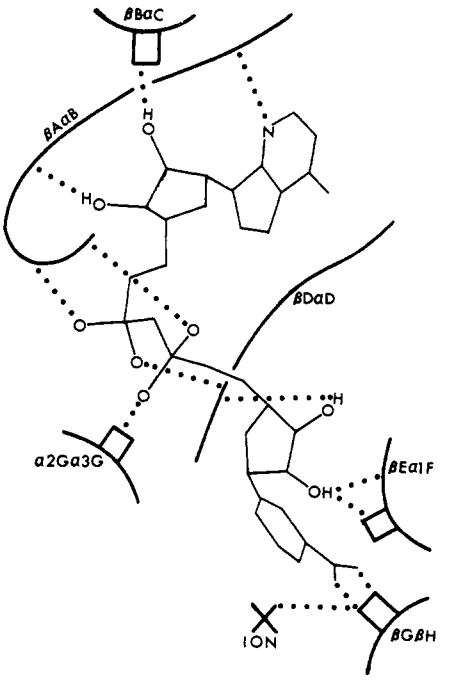

FIGURE 8: Schematic diagram of interactions between NAD^+ and malate dehydrogenase. Nomenclature for the protein segments is explained in the text. Dotted lines indicate possible hydrogen bonds. Rectangles indicate side chains large enough to be clearly visible in the electron density map. The position assigned to a sulfate ion is also shown.

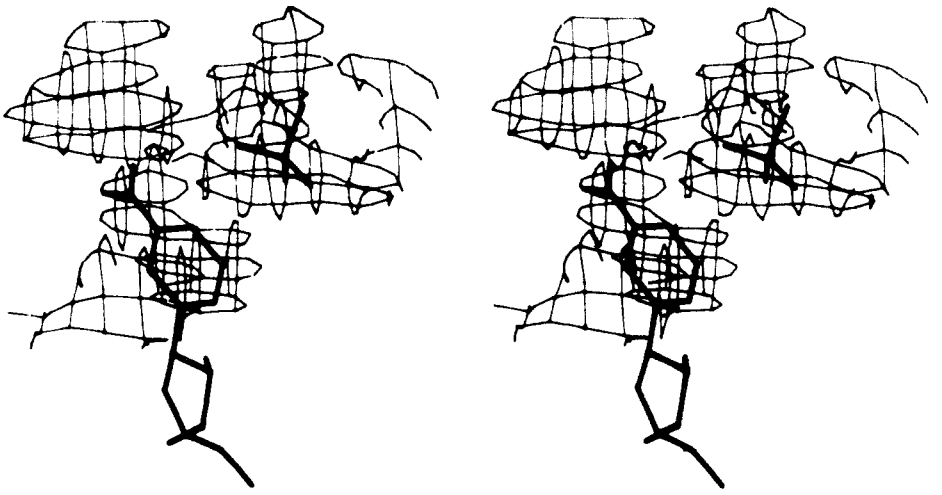

FIGURE 9: Nicotinamide ring and sulfate ion bound to subunit 1 with related regions of the malate dehydrogenase 2.5-Å resolution electron density map. The contours were generated as in Figure 4, and some of the electron density belonging to side chains near the sulfate ion has been suppressed so that the large peak containing this ion is clearly visible. The sulfate ion has been placed in an arbitrary orientation in this electron density.

the segments of peptide chain has been adopted for both lactate and malate dehydrogenases (Hill *et al.*, 1972). The prefixes α and β specify α helices and β structure. Turns are represented by combinations representing the segments connected. For example, the βDαD segment, also called the "loop," joins the βD strand and the αD helix. Although hydrogen bonds cannot be specified until the malate dehydrogenase sequence is known, it is clear that most of the contacts specified by the dotted lines are close enough to implicate this type of bonding.

Comparison of the malate dehydrogenase electron density map with a recent detailed description of hydrogen bonding between NAD^+ and lactate dehydrogenase (Adams *et al.*, 1973a) reveals that side chains in structurally homologous regions bind the dinucleotide in the malate dehydrogenase. For example, the 2′-hydroxyl group of the adenine ribose in malate dehydrogenase is probably hydrogen bonded to a side chain in the βBαC turn. The same ribose hydroxyl group hydrogen bonds to Asp-53 in lactate dehydrogenase, a residue also in the βBαC turn. In both enzymes, a residue at the end of the α2Gα3G turn is involved in binding to one of the oxygens on the nicotinamide phosphorus atom. In malate dehydrogenase, the 2′-OH group in the nicotinamide ribose is implicated in hydrogen bonding to the βEα1F turn, either to the main chain itself, as in lactate dehydrogenase, or to a large side chain. The electron density of this side chain at βEα1F lies over the nicotinamide ring in the same way as Glu-140, in the homologous turn in lactate dehydrogenase, approaches the reactive A side of this ring. As in lactate dehydrogenase, the loop residues in malate dehydrogenase play an important role in binding the nicotinamide ribose 3′-hydroxyl group and/or the phosphorus oxygens.

However, some of the residues which are hydrogen bonded to the dinucleotide in lactate dehydrogenase are much further removed from the coenzyme in malate dehydrogenase, and it should be emphasized that substantial differences must exist, especially in the active-site region. The nicotinamide ring of subunit 1 and the related regions of the malate dehydrogenase electron density map are shown in Figure 9. The density directly behind the nicotinamide ring belongs to the βEα1F side chain discussed above. The large peak ascribed to a sulfate ion is close to the nicotinamide C-4 atom and several large side chains. The ion site is present in both subunits and is positioned in a homologous manner to the anion location in the active site of dogfish lactate dehydrogenase (Adams *et al.*, 1973b). The presence of this ion close to the C-4 atom on the A side of the nicotinamide ring suggests, of course, that the removal of the ion is a necessary step in the reaction mechanism.

The position of the carboxamide group between the nicotinamide ring and a large nearby side chain is marked by a large region of electron density. The conformation about the C-3–C-7 bond cannot be determined at this resolution; the amide group has been twisted 24° from the plane of the ring in accordance with the crystal-structure determination of nicotinamide (Wright and King, 1954). The side chain which approaches and apparently hydrogen bonds to the carboxamide group has been tentatively assigned to the βGβH turn and is shown schematically in Figure 8. This assignment puts this side chain in a position homologous to that occupied by an essential histidine in lactate dehydrogenase, identified as His-195 (Adams *et al.*, 1973b).

A complete interpretation of the binding of NAD^+ to malate dehydrogenase must include relevant changes of conformation between the two protein subunits. Significant differences in the loop region of the two subunits have been noted. It is clear also that the loop region in both subunits of the malate dehydrogenase binary complex has a conformation substantially different from that of the loop in dogfish lactate dehydrogenase apoenzyme. The malate dehydrogenase loop resembles somewhat more closely the loop in the lactate dehydrogenase ternary complex, which is folded down over the coenzyme and substrate (Adams *et al.*, 1972). The differences noted between the loop positions in the two malate dehydrogenase subunits can be documented in detail when the model of the polypeptide backbone for both subunits is complete.

Acknowledgment

We are grateful to Drs. C. D. Barry and J. Fritsch for helpful suggestions on the conformational analysis and the molecular modeling system and to Dr. D. Tsernoglou for his work in the early stages of this study. We also acknowledge the assistance of Drs. M. Rossmann, A. Liljas, and M. Hackert in comparing the binding of coenzyme to lactate dehydrogenase and malate dehydrogenase. The authors are grateful to Dr. R.

Bradshaw and Dr. B. Glatthaar for helpful discussions on the chemistry of dehydrogenases and to Mr. G. Barbarash and Mr. E. Puronen for their excellent technical assistance.

References

Adams, M. J., Buehner, M., Chandrasekhar, K., Ford, G. C., Hackert, M. L., Liljas, A., Lentz, P., Jr., Rao, S. T., Rossmann, M. G., Smiley, I. E., and White, J. L. (1972), *in* Protein–Protein Interactions, Bergmann, E., and Pullmann, B., Ed., Berlin, Springer-Verlag, p 139.

Adams, M. J., Buehner, M., Chandrasekhar, K., Ford, G. C., Hackert, M. L., Liljas, A., Rossmann, M. G., Smiley, I. E., Allison, W. S., Everse, J., Kaplan, N. O., and Taylor, S. S. (1973a), *Proc. Nat. Acad. Sci. U. S. 70*, 1968.

Adams, M. J., Ford, G. C., Koekoek, R., Lentz, P. J., Jr., McPherson, A., Jr., Rossmann, M. G., Smiley, I. E., Schevitz, R. W., and Wonacott, A. J. (1970a), *Nature (London) 227*, 1098.

Adams, M. J., Liljas, A., and Rossmann, M. G. (1973b), *J. Mol. Biol. 76*, 519.

Adams, M. J., McPherson, A., Jr., Rossmann, M. G., Schevitz, R. W., and Wonacott, A. J. (1970b), *J. Mol. Biol. 51*, 31.

Arnott, S., and Hukins, D. W. L. (1969), *Nature (London) 224*, 886.

Barry, C. D., North, A. C. T., Glasel, J. A., Williams, R. J. P., and Xavier, A. V. (1971), *Nature (London) 232*, 236.

Bruice, J. C., and Benkovic, S. J. (1966), Bioorganic Mechanisms, Vol. II, New York, N. Y., W. A. Benjamin, Chapter 9.

Chandrasekhar, K., McPherson, A., Jr., Adams, M. J., and Rossmann, M. G. (1973), *J. Mol. Biol. 76*, 503.

Davies, D. D., Teixeira, A., and Kenworthy, P. (1972), *Biochem. J. 127*, 335.

Glatthaar, B. E., Banaszak, L. J., and Bradshaw, R. A. (1972), *Biochem. Biophys. Res. Commun. 46*, 757.

Hill, E., Tsernoglou, D., Webb, L., Banaszak, L. J., Jacobi, T., Ellis, R., and Fritsch, J. (1972), *J. Mol. Biol. 72*, 577.

Levy, H. R., and Vennesland, B. (1957), *J. Biol. Chem. 228*, 85.

McDonald, G., Brown, B., Hollis, D., and Walter, C. (1972), *Biochemistry 11*, 1920.

Pletcher, J., and Sax, M. (1966), *Science 154*, 1331.

Richards, F. M. (1968), *J. Mol. Biol. 37*, 225.

Rossmann, M. G., Adams, M. J., Buehner, M., Ford, G. C., Hackert, M. L., Lentz, P. J., Jr., McPherson, A., Jr., Schevitz, R. W., and Smiley, I. E. (1971), *Cold Spring Harbor Symp. Quant. Biol. 36*, 179.

Sundaralingam, M. (1969), *Biopolymers 7*, 821.

Sundaralingam, M. (1973), *in* Symposia on Quantum Chemistry and Biochemistry, Vol. V, Bergmann, E., and Pullman, B., Ed., Jerusalem, Israel Academy of Sciences and Humanities, pp 417–456.

Tsernoglou, D., Hill, E., and Banaszak, L. J. (1971), *Cold Spring Harbor Symp. Quant. Biol. 36*, 171.

Wright, W. B., and King, G. S. D. (1954), *Acta Crystallogr. 7*, 283.

Vitamin B_6 Catalysis. α-Phenylaminomalonate-Catalyzed Reactions of 5-Deoxypyridoxal†

John W. Thanassi

ABSTRACT: The pH–rate profile for the decarboxylation of α-phenylaminomalonic acid has been determined and describes a bell-shaped curve. The reactive species is the neutral, zwitterionic form, $+NH_3C_6H_5(COOH)COO^-$, which decarboxylates approximately 5×10^6 times more readily than malonic acid monoanion, $CH_2(COOH)COO^-$. The products from the reaction of α-phenylaminomalonate and 5-deoxypyridoxal at pH 5.2 were separated by ion-exchange chromatography and were identified as 5-deoxypyridoxamine, a dimer incorporating one molecule of 5-deoxypyridoxamine and one molecule of 5-deoxypyridoxal (compound J), and a diastereoisomer of compound J (compound K). The reactions of 5-deoxypyridoxal with aminomalonic acid, α-methylaminomalonic acid, and α-phenylaminomalonic acid are compared, and discussed in terms of the mechanism of vitamin B_6 catalysis, with reference to electronic and steric control factors.

Aminomalonic acid, $NH_2CH(COOH)_2$, and its derivatives are interesting compounds on both chemical and biochemical grounds. This amino acid was utilized by Ogsten (1948) to illustrate his theoretical arguments that enzymes can in fact distinguish groups on apparently symmetrical, optically inactive, molecules of the type C (a,b,d,d). Ogsten's publication led to greater insights on the stereochemistry of enzyme-catalyzed reactions and had the important consequence of reinstating citric acid as an intermediate in the tricarboxylic acid cycle of glucose oxidation. A possible biological role for aminomalonic acid as an intermediate in the serine to glycine conversion was proposed about 60 years ago by Knoop (1914) and was later explored by Shemin (1946). More recently, aminomalonic decarboxylase activity from silkworm glands (Shimura *et al.*, 1956) and rat liver (Thanassi and Fruton, 1963) has been reported, leading to further speculation on potential roles for aminomalonic acid in intermediary metabolism (Meister, 1965). However, the possibility of a biological role for aminomalonic acid appears to have been laid to rest in a recent publication by Palekar *et al.* (1973) who demon-

† From the Department of Biochemistry, University of Vermont, College of Medicine, Burlington, Vermont 05401. *Received July 9, 1973.* These studies were supported by U. S. Public Health Service Grant No. 5-R01-AM12436.